

Numerical model of magnetic fluid hyperthermia

Abstract. The article presents the computer model of magnetic fluid hyperthermia (MFH), which is new, promising cancer treatment. Special attention was focused on the complete mapping of physical and biological phenomenon, such as a realistic model of magnetic field excitement, blood perfusion, metabolic heat and convective heat exchange with the environment. The described model was implemented using the finite element method.

Streszczenie. Artykuł prezentuje metodę numerycznego modelowania hipertermii płynu magnetycznego (ang. MFH), która jest nową, obiecującą techniką leczenia nowotworów. Specjalna uwaga została zwrócona na pełne odwzorowanie zjawisk fizycznych i biologicznych, takich jak: realistyczny model wymuszenia magnetycznego, zjawisko perfuzji krwi, metaboliczne źródła ciepła oraz zjawisko konwekcyjne wymiany ciepła z otoczeniem. Opisany model został zaimplementowany przy wykorzystaniu metody elementów skończonych. **Numeryczny model hipertermii płynu magnetycznego**

Keywords: Magnetic Fluid Hyperthermia, computational bioelectromagnetics, superparamagnetic heat

Słowa kluczowe: Hipertermia płynu magnetycznego, bioelektromagnetyzm obliczeniowy, grzanie superparamagnetyczne

Introduction

According to the reports made by National Cancer Registry and Polish Committee for Fighting Cancer, cancer is the second after circulatory system diseases cause of death in Poland. Among different types of cancer, the most frequent malignant tumor observed in active women in age between 40 and 60 is the breast cancer.

Breast cancer diagnosed early enough, i.e. the diameter of cancer is lower than 2 cm, can be treated successfully in 90 percent of cases. That implicates the possibility of a minimal-invasive treatment without deformation of the morphological structure of the organ is of special interest for the patient's emotional and physical welfare. One of such methods, being developed nowadays, is hyperthermia. Human cells are very sensitive to temperature. Heating body above 42°C activates cellular self-destruction mechanism, in biology called apoptosis. This phenomenon underlies the hyperthermia therapy for cancer treatment [3],[11].

The hyperthermia treatment has shown its effectiveness not only for breast cancer, but more generally for patients where tumor is found in one well-defined location [6]. Different technologies are used to heat up the malicious tissue, such as focused ultrasound, infrared sauna, microwave heating, induction heating, magnetic hyperthermia, infusion of warmed liquids, or direct contact.

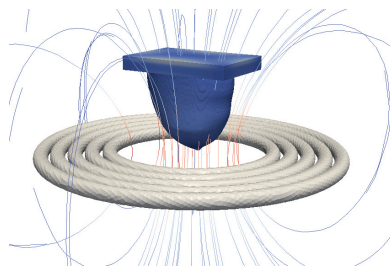


Fig. 1. Excitation coil generates time-varying magnetic field, which is a source of paramagnetic heat inside the body

The main concern of hyperthermia is to provide well-controlled and localized heat source directly to the cancerous tissue. One of the best methods to focus heat on the tumor is Magnetic Fluid Hyperthermia (MFH), where magnetic particles are injected directly into the place of interest. The general idea of MFH (see Fig. 1) is that external magnetic field generates a therapeutic temperature by the use of superparamagnetic heating only inside the tumor without threats for the rest of the body. On the one hand the authors [2], [5], [8] aim to estimate the amount of magnetic fluid needed in hyperthermia treatment as a function of nanoparticles optimal

diameter, cancer size and optimal concentration. On the other hand Computer Aid Diagnosis and numerical methods concerning the issue have to be developed. In this paper the authors are presenting the complete mathematical model of MFH treatment taking into account: realistic coil shape, conductive and superparamagnetic heating phenomenon, blood perfusion factor and convective skin cooling. Furthermore, selected important aspects of numerical algorithms and their application with the use Finite Element Method (FEM) are discussed.

Mathematical description

The magnetic fluid hyperthermia is a complicated multi-physics problem, which is covered by two partially independent solutions: one for magnetic field solution and the second one for heat transfer equation [1].

When low frequency (150 kHz) electromagnetic field is taken into consideration magnetic field near the coil is highly dominant. Thus, the electric field can be neglected and on the base of quasi-static model and vector Laplace operator for magnetic vector potential (\mathbf{A}) one can get:

$$(1) \quad -\nabla^2 \mathbf{A} = \mu_0 \mathbf{J}$$

The generated magnetic field ($\mathbf{H} = 1/\mu_0 \nabla \times \mathbf{A}$) stimulates both, superparamagnetic and conductive heat. The first one is based on Néelian and Brownian mechanisms of relaxation and the related power density can be expressed by formula [10]:

$$(2) \quad p_{mf} = \pi \mu_0 \chi_0 \mathbf{H}^2 f \frac{2\pi f \tau}{1 + (2\pi f \tau)^2},$$

where f is the frequency of H-field, χ_0 is the susceptibility of magnetic fluid, τ is the particle relaxation time. The second one is classical eddy current approach connected directly with current density \mathbf{J} flowing inside the body. Power loss density p can be described by well known formula:

$$(3) \quad p = \frac{1}{\sigma} \mathbf{J}^2$$

where σ is the conductivity [S/m].

To find the distribution of current density inside the body the quasi-static equation for scalar electric potential u has to be solved:

$$(4) \quad -\nabla \cdot (\sigma \nabla u) = \nabla \cdot (\sigma 2\pi f \mathbf{A}),$$

then \mathbf{J} can be express as

$$(5) \quad \mathbf{J} = -\sigma \nabla u - \sigma(2\pi f \mathbf{A})$$

Finally, in order to combine the eddy currents conductive losses and superparamagnetic heat generated inside magnetic fluid, one should include the concentration (θ) of magnetic nanoparticles inside the subdomain under consideration, which leads to

$$(6) \quad Q_{MH} = p + \theta p_{mf},$$

where Q_{MH} is often called external power density.

Having identified all the factors connected with magnetic field the next step is to find the temperature distribution. In 1948 Henry H. Pennes performed medical experiments which led him to expanding simple heat equation by effects of metabolic heat and blood perfusion discovery. In our model we have taken advantage of this classical study. Nowadays the formula (7) is called Pennes equation:

$$(7) \quad \rho c \frac{\partial T}{\partial t} = \nabla \cdot (k \nabla T) + \rho_b c_b \omega (T_b - T) + Q_{met} + Q_{MH}$$

where ρ is tissue density [kg/m^3], c - tissue specific heat [$\text{J}/\text{kg}/\text{K}$], ρ_b - density of blood [kg/m^3], c_b - blood specific heat [$\text{J}/\text{kg}/\text{K}$], k - tissue thermal conductivity [$\text{W}/\text{m}/\text{K}$], ω - blood perfusion rate [1/s], T_b - arterial blood temperature [K], Q_{met} - metabolic heat source [W/m^3].

Another important factor of MFH is the cooling associated with heat exchange with the environment. This can be described by a convection and imposed in the form of Robin boundary condition: $\frac{\partial T}{\partial n} = h(T_{ext} - T)$,

where h is the heat transfer coefficient [$\text{W}/\text{m}^2/\text{K}$] and T_{ext} is the external temperature.

Homogeneous composite

A mathematical description of living tissues properties is a challenging task. Since simulation results are very fragile for the properties of materials, one has to carefully select these data. Most of these values can be found in the literature, but we have to be aware of significant discrepancies among them.

Table 1. Formulas used for homogeneous mixture of two materials

density	$\rho = (1 - \theta)\rho_1 + \theta\rho_2$
specific heat	$c = (1 - \theta)c_1 + \theta c_2$
thermal conductivity	$\kappa = (\kappa_1 \kappa_2) / ((1 - \theta)\kappa_2 + \theta \kappa_1)$
electrical conductivity	$\sigma = (\sigma_1 \sigma_2) / ((1 - \theta)\sigma_2 + \theta \sigma_1)$

In our simulations, we used the parameters of magnetite (Fe_2O_3) [10], which is a popular magnetic material with strong magnetic properties and low toxicity [4]. Magnetite coated with surfactant agents is an ingredient of magnetic fluid, which injected into the tumor, significantly changes its properties. For the values of homogeneous composite we have used equations presented in Table 1.

Numerical model

To simulate the processes of MFH, the authors have taken advantage of FEM C++ software package FEniCS [7]. It is the open-source project developed by scientific community around the world. The main concept behind FEniCS is the automatization of scientific computing, which is achieved by assembling specialized numerical open-source libraries and by providing convenient way to solve a wide class of FEM problems. The major novelty lies in advancing Finite

Element Form Language (UFL) [7]. Using UFL is directly related to mathematical weak form formulation, which is a natural way of describing PDE problems as follows:

$$(9) \quad a(u, v) = L(v)$$

where $a(u, v)$ is known as a bilinear form and $L(v)$ as a linear form.

To demonstrate the use of UFL language the equation (1) has been chosen. Multiplying both sides by the vector test function \mathbf{v} yields

$$(10) \quad -(\nabla^2 \mathbf{A}) \cdot \mathbf{v} = \mu_0 \mathbf{J} \cdot \mathbf{v}$$

Since the two functions are equal on Ω , their integrals over Ω must agree:

$$(11) \quad - \int_{\Omega} (\nabla^2 \mathbf{A}) \cdot \mathbf{v} \, dx = \int_{\Omega} \mu_0 \mathbf{J} \cdot \mathbf{v} \, dx$$

Applying Green's identity to the left side gives

$$(12) \quad - \int_{\Omega} (\nabla^2 \mathbf{A}) \cdot \mathbf{v} \, dx = \int_{\Omega} \nabla \mathbf{A} \cdot \nabla \mathbf{v} \, dx - \int_{\Gamma} \mathbf{v} \frac{\partial \mathbf{A}}{\partial n} \, ds$$

The boundary integral vanishes when \mathbf{A} is a solution of (1), since $\partial \mathbf{A} / \partial n$ is zero on Γ . Finally, the weak form is as follows:

$$(13) \quad \int_{\Omega} (\nabla \mathbf{A} \cdot \nabla \mathbf{v}) \, dx = \int_{\Omega} \mu_0 (\mathbf{J} \cdot \mathbf{v}) \, dx$$

Having equation (13) in the form presented in (9) one can use UFL language as follows:

```
#Continuous Galerkin, linear Lagrange element
eN = VectorElement("CG", "tetrahedron", 1)

#Discontinuous Galerkin, degree 0
eL = VectorElement("DG", "tetrahedron", 0)

v = TestFunction(eN)
A = TrialFunction(eN)
J = Coefficient(eL)
mu0 = Constant("tetrahedron")

a = inner(grad(A), grad(v)) * dx
L = mu0 * inner(J, v) * dx
```

A detailed discussion of every PDE problem presented in the paper definitely exceeds its volume but unlike equations from (1) to (6), which can be solved using presented above pattern, Pennes equation (7) with boundary condition (8) has to be solved in the time domain. Fortunately the equation is very stable (see Fig. 2), and it can be solved by backward Euler scheme with a fixed time step.

After introducing the backward Euler scheme, multiplication by test function v and integration over domain Ω bounded by Γ , we obtain needed bilinear variational form $a(T, v)$:

$$\int_{\Omega} (\rho c T v + \delta_t \kappa (\nabla T \cdot \nabla v) + \delta_t \rho_b c_b \omega T v) \, dx + \int_{\Gamma} h T v \, ds$$

and linear variational form $L(v)$:

$$\int_{\Omega} (\delta_t T_{ext} + \delta_t (Q_{ext} + Q_{met}) + \delta_t \rho_b c_b \omega T_b) v \, dx +$$

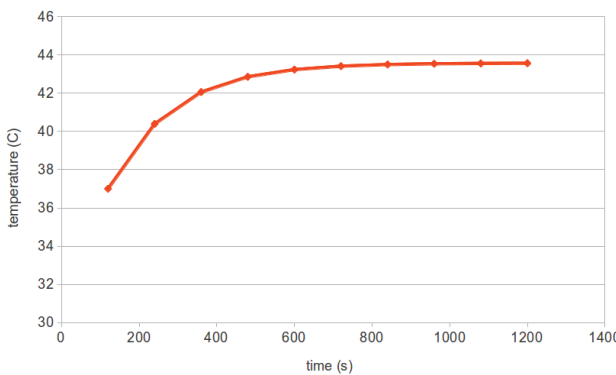


Fig. 2. Typical temperature time plot. Saturation effect is related to the blood perfusion.

$$\begin{aligned}
 a &= (\rho \cdot c \cdot T \cdot v + dt \cdot \kappa \cdot \text{inner}(\text{grad}(T), \\
 &\quad \text{grad}(v)) + dt \cdot \rho_b \cdot c_b \cdot \omega \cdot T \cdot v) \cdot dx \\
 &\quad + h \cdot T \cdot v \cdot ds \\
 L &= (\rho \cdot c \cdot T_0 + dt \cdot (Q_{ext} + Q_{met}) \\
 &\quad + dt \cdot \rho_b \cdot c_b \cdot \omega \cdot T_b) \cdot v \cdot dx \\
 &\quad + h \cdot T_{ext} \cdot v \cdot ds
 \end{aligned}$$

Simulations

Although the paper is devoted to the mathematical and numerical description of MFH, the simple demonstration of the method will be included.



Fig. 3. Four anatomical breast models. One for each class according to the Numerical Breast Phantoms Repository [9] (from left: mostly fatty, scattered fibroglandular, heterogeneously dense, very dense).

On the base of online repository named Numerical Breast Phantoms Repository [9], which provides a database of anatomically realistic numerical breast phantoms, the authors have prepared four different models with regard to their shapes as it is shown in Fig. 3. Each phantom includes 1.5 mm thick skin layer, 1.5 cm thick fat layer as the base of the the breast and 0.5 cm thick muscle chest wall. In our case we have also implemented 2 cm diameter tumor layer to every model.

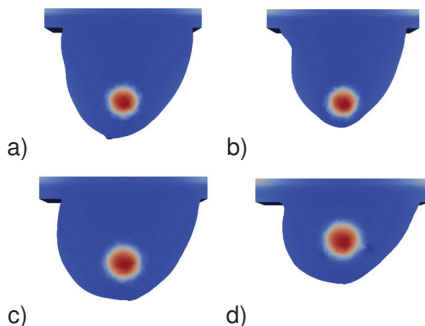


Fig. 4. Temperature distribution in each breast phantom after 30-minute of continuous heating. The stimulation coil is located with the same distance to the tumor. Color scale is equal for every picture.

Simulation software running on a standard workstation computer was able to solve realistic breast models (consists of $150 \cdot 10^3$ elements) in less than 5 minutes. Approximately half of the time was taken by quasi-static solver for the heat

sources (Q_{MH}), and the other half of the time took the time domain temperature simulator.

The results of a 30-minute exposition are shown in Fig. 4. To investigate the influence of breast shape and structure on MFH performance, the tumor was located in the same distance to the stimulation coil and loaded with the same concentration (θ). As it is seen in pictures a), b), c), d) (the same color scale) maximum temperature values were exactly the same and amount to 43.6°C .

To conclude this simple demonstration experiment, the authors can state that MFH therapy definitely will not be influenced by the breast class and shape.

Conclusions

This paper has presented the mathematical description and the multi-step numerical simulation of magnetic fluid hyperthermia. The model was developed so as to take into account as many aspects of reality as possible: 3D shapes of coil and body model, conductive and superparamagnetic heating, blood perfusion and convective skin cooling.

Finite element solver was implemented using FEniCS library, which proved to be an elegant and efficient solution for multi-physics, advanced simulations. The authors are convinced that the developed simulator will be useful in therapy planning.

BIBLIOGRAPHY

- [1] A. Candeo and F. Dughiero: Numerical FEM Models for the Planning of Magnetic Induction Hyperthermia Treatments with Nanoparticles, *IEEE Transactions on Magnetics*, vol. 45, no. 3, March 2009, pp. 1658–1661
- [2] P. Di Barba, F. Dughiero and E. Sieni: Magnetic Field Synthesis in the Design of Inductors for Magnetic Fluid Hyperthermia, *IEEE Transactions On Magnetics*, Vol. 46, No. 8, 2010, pp. 2931–2934
- [3] P. Gas: Essential Facts on the History of Hyperthermia and their Connections with Electromedicine, *Electrical Review*, 87(2011), No. 12b, 37–40.
- [4] R. Hergt, S. Dutz, R. Muller and M. Zeisberger: Magnetic particle hyperthermia: nanoparticle magnetism and materials development for cancer therapy, *J. Phys.: Condens. Matter* 18, 2006, pp. S2919–S2934.
- [5] R. Kappiyoor, M. Liangruksa, R. Ganguly, and I. K. Puri: The effects of magnetic nanoparticle properties on magnetic fluid hyperthermia, *Journal Of Applied Physics* 108, 094702, 2010.
- [6] E. Kurgan, P. Gas: Treatment of tumors located in the human thigh using RF hyperthermia, *Electrical Review (Przeglad Elektrotechniczny)*, vol. 87, No 12b, 2011, pp. 103–106.
- [7] A. Logg, K.-A. Mardal, G. N. Wells et al.: Automated Solution of Differential Equations by the Finite Element Method, Springer, 2012
- [8] A. Miaskowski, B. Sawicki, A. Krawczyk: The use of magnetic nanoparticles in low frequency inductive hyperthermia, *COMPEL*, Vol. 31 No. 4, 2012, pp. 1096–1104
- [9] UWCEM Numerical Breast Phantoms Repository, <http://uwcem.ece.wisc.edu/home.htm>
- [10] R. E. Rosensweig, Heating magnetic fluid with alternating magnetic field (2002), *Journal of Magnetism and Magnetic Materials* Vol. 252, pp. 370–374
- [11] P. Wust, B. Hildebrandt, G. Sreenivasa, B. Rau, J. Gellermann, H. Riess, R. Felix, and P.M. Schlag: Hyperthermia in combined treatment of cancer, *The Lancet - Oncology*, Vol 3, August 2002, pp.487-497

Authors: Bartosz Sawicki, Institute of Theory of Electrical Engineering, Measurement and Information Systems, Faculty of Electrical Engineering, Warsaw University of Technology, ul. Koszykowa 75, 00-662 Warszawa, Poland, email: sawickib@iem.pw.edu.pl. Arkadiusz Miaskowski, Department of Applied Mathematics and Computer Science, University of Life Sciences in Lublin, Akademicka 13, 20-950 Lublin, Poland, email: